

Manuscript version: Author's Accepted Manuscript

The version presented in WRAP is the author's accepted manuscript and may differ from the published version or Version of Record.

Persistent WRAP URL:

<http://wrap.warwick.ac.uk/111548>

How to cite:

Please refer to published version for the most recent bibliographic citation information. If a published version is known of, the repository item page linked to above, will contain details on accessing it.

Copyright and reuse:

The Warwick Research Archive Portal (WRAP) makes this work by researchers of the University of Warwick available open access under the following conditions.

© 2018, Elsevier. Licensed under the Creative Commons Attribution-NonCommercial-NoDerivatives 4.0 International <http://creativecommons.org/licenses/by-nc-nd/4.0/>.



Publisher's statement:

Please refer to the repository item page, publisher's statement section, for further information.

For more information, please contact the WRAP Team at: wrap@warwick.ac.uk.

Photo-Polymerisation and Study of the Ice Recrystallisation Inhibition of Hydrophobically Modified Poly(vinyl pyrrolidone) Co-polymers

Christopher Stubbs,^a Thomas R Congdon,^a Matthew I. Gibson*^{a,b}

^a Department of Chemistry, University of Warwick, UK CV4 7AL

^b Warwick Medical School, University of Warwick, UK CV4 7AL

* Corresponding author. Email m.i.gibson@warwick.ac.uk

Abstract

Antifreeze, ice binding and ice nucleating proteins modulate the formation and growth of ice in biological systems, enabling extremophiles to survive in sub-zero temperatures. A common feature is their rigidity, and segregated hydrophobic and hydrophilic domains. It has been demonstrated that increased hydrophobicity in rigid, facially amphipathic, synthetic polymers enhances ice recrystallisation inhibition (IRI) activity, but has not been evaluated in flexible systems. Here photochemical RAFT/MADIX polymerisation is used to obtain well-defined poly(*N*-vinyl pyrrolidone), PVP, copolymers to probe the impact of hydrophobicity on ice recrystallisation inhibition in a fully flexible polymer system, to increase the understanding on how to mimic antifreeze proteins. It is observed that PVP homopolymers have only very weak, molecular weight dependent, IRI and that hydrophobic co-monomers give very modest changes in IRI, demonstrating that the spacial segregation of ‘philicities’ is crucial, and not just the overall hydrophobic content of the polymer. These results will help design the next generation of IRI active polymers for cryopreservation applications as well as aid our understanding of how biomacromolecules can inhibit ice growth.

Keywords

Photo Chemistry, Polymers, Ice growth Inhibition, Post-polymerisation Modification

Introduction

The formation and growth of ice is a major problem in the engineering,¹ aerospace,² and medical^{3,4} fields. Nature has evolved a diverse series of biomacromolecules which can prevent or promote ice formation⁵⁻⁷ or prevent seeded ice crystals from growing further.^{8,9} Ice growth (recrystallisation) is a particular issue in the cryopreservation of cells,^{10,11} contributing to cell death post-thaw and hence any materials (biological or synthetic) which can modulate this may find a role within the biological cold-chain, including emerging cell-based therapies¹²⁻¹⁵ and also for proteins¹⁶ and bacteria.¹⁷ Synthetic polymers which can mimic the function of antifreeze (glyco)proteins (AF(G)Ps) have emerged,¹⁸⁻²⁰ especially ice recrystallisation inhibition (IRI), but the design rules to enable the discovery of new materials remain elusive. Simulations suggest AF(G)Ps bind to the prism plane of ice *via* hydrophobic interactions with their backbone.²¹ However, Budke and Koop found low IRI activity of the AFGP backbone when the saccharide moieties were removed,²² and other groups have proposed other modes of action, which have been summarised by Ben and coworkers.⁹ AFPs appear to bind *via* an ‘anchored clathrate’ mechanism, using pre-ordered water molecules,²³ but there is computational²⁴ and experimental²⁵ evidence for the effect that hydrophobic surfaces on the protein have in ice binding. The most IRI active synthetic macromolecule identified to date is poly(vinyl alcohol)^{26,27} which has few structural similarities to either AFP or AFGP, and recent results support a distinct mechanism involving hydrogen bonding *via* a precise spacing match between hydroxyls on the PVA chain and the prism plane of ice.^{28,29} Drori *et al.* have demonstrated that safranin O can self-assemble into fibres leading to remarkable IRI and ice shaping ability³⁰ highlighting that there are potentially many mechanisms of interaction with a growing ice face which may lead to the macroscopic effect of ice growth inhibition. [It is important to distinguish growth from nucleation promotion/inhibition, which is a distinct process]. A common feature of all IRI active materials (large or small molecules) is that they have a balance between hydrophilic and

hydrophobic contributions which seems to be essential, or at least highly desirable. Mitchell *et al.* showed that self-assembled metallohelices were potent IRIs despite having no obvious hydrogen bonding motifs, and that the most active had segregated hydrophilic and hydrophobic domains across their surface.³¹ Facially amphiphilic rigid glycopolymers (derived from ROMP polymerisation) have definite IRI activity (50% or greater inhibition of ice growth),³² in contrast to fully flexible glycopolymers from methacrylate monomers³³ which can freely rotate around the backbone, supporting the need for segregated ‘philicities’ for at least one mechanism of ice growth inhibition. Hydroxyl groups (as in PVA) are also not essential; Ben *et al.* have developed lysine derivatives where IRI activity increases with hydrophobicity, but not with the critical micelle concentration, ruling out micellisation as a factor.^{34,35} Crucially, these compounds do not lead to ice shaping, implying that ice-face binding may not be essential for inhibiting growth, but instead limiting the rate of exchange at the quasi liquid layer,³⁶ although this has not been proven yet.

The challenging nature of the ice-water interface and the lack of understanding of ice nucleation makes the rational design of new polymeric AF(G)P mimics challenging.³⁷ In contrast to ice inhibition, there are many examples of kinetic hydrate inhibitors (KHI) for gas hydrates, with polymers containing amides being particularly important^{38,39} including poly(*N*-vinyl pyrrolidone). This suggests that vinyl lactams maybe good candidates for exploring new IRI active polymers. Many KHI are based on lesser activated monomers (LAMs) which are more challenging to polymerise by controlled radical polymerisation. The radical created during initiation and propagation is much more reactive than the monomer itself, leading to a variety of side reactions during the polymerisation, with a high propensity for chain transfer to both solvent and monomer.⁴⁰ In a conventional RAFT polymerisation, the conjugation of the RAFT agent would be enough to generate a stable material, leading to the end of the polymerisation reaction. The addition of a much less stable Z group is required in order to prevent this deactivation, and thus xanthates, *N*-aryl dithiocarbonates, or

dithionaphthalates,⁴¹ which provide less stability to the radical are required, as opposed to the usual di- or tri- thiocarbonates.⁴²

Photopolymerisation is a rapidly emerging tool in polymer synthesis enabling temporal control and enabling milder reaction conditions compared to traditional thermal initiation methods.^{43,44} Xanthates have been reported to enable RAFT/MADIX polymerisation of LAMs using visible light *via* direct photolysis,⁴⁵ but also by photoredox catalysis known as photoinduced electron-transfer: PET-RAFT.⁴⁶ A particular advantage of these photochemical methods is the ability to conduct the polymerization in the presence of oxygen⁴⁷⁻⁴⁹ and at room temperature which helps avoid the thermally-induced side reactions associated with high temperature polymerisation of vinyl acetate, for example.⁵⁰

It is currently not clear if vinyl lactams could be repurposed for ice growth inhibition, inspired by their use as kinetic hydrate inhibitors. Considering this, the aim of this work was to systematically explore if the ice recrystallisation activity of PVPs homopolymer could be modulated through the introduction of statistically distributed hydrophobic groups. Photo-RAFT polymerisation was used for the first time to obtain poly(*N*-vinyl pyrrolidone), and copolymers with poly(vinyl acetate) at room temperature. After deprotection of the acetate groups, esterification enabled the introduction of a range of side chains, whilst ensuring identical molecular weight distributions. IRI activity measurements showed that IRI activity was not achieved, confirming that local rigidity and facial amphiphilicity are crucial, rather than just the addition of a simple hydrophobic comonomer.

Results and Discussion

Intrinsic photo-RAFT/MADIX (using blue LEDs)^{47,51} was chosen, as opposed to thermal RAFT for the polymerisation of vinyl pyrrolidone, as it removes the need for a separate radical source (e.g. AIBN) and allows polymerisation to be conducted at room temperature. This polymerisation mechanism appears to have characteristics of an iniferter process rather than pure RAFT mechanism, with the blue light photolyzing the xanthate to generate radicals.⁵² Ethyl 2-((ethoxycarbonothioyl)thio)propanoate has previously been shown to initiate and control the polymerisation of vinyl acetate using only blue light and hence was the starting point.⁵³ In this work, the methyl ester derivative was synthesised from commercially available potassium ethyl xanthate and 2-methyl bromopropionate, and this was used for all polymerisations (see ESI for synthesis), due to its facile synthesis/purification. Initial attempts to polymerise *N*-vinyl pyrrolidone by photo-RAFT/MADIX under blue light without deoxygenation using a tertiary amine oxygen scavenger^{47,51} failed to afford polymer and was not explored further. To overcome this, bulk solutions of monomer/CTA were placed in the reaction vessel and first degassed using N₂, and then subjected to blue light, Figure 1A. In our screening we observed that this led to polymer formation at room temperature (with no added initiator), and that the polymers typically had lower dispersities (< 1.3 compared to 1.6 by conventional RAFT²⁶). To the authors' knowledge this is the first example of VP photopolymerisation using a direct photolysis RAFT agent. A panel of PVP homopolymers with targeted degrees of polymerisation from 25 to 100 were obtained using this method. SEC molecular weights were larger than expected, as is commonly seen for PVP, which is difficult to accurately measure in SEC, as it has unusual elution behaviour in commonly used solvents^{26,54,55} (other than hexafluoro-isopropanol⁵⁶) Figure 1B.

Table 1. PVP homopolymers synthesised in this work

Sample ^a	[VP]:[CTA] ^b (-)	Conv ^c (%)	Mn _{Theo} ^d (g.mol ⁻¹)	Mn _{SEC} ^e (g.mol ⁻¹)	Đ ^e (-)
PVP ₁₄	20	44	980	1500	1.22
PVP ₂₉	50	N/A ^f	N/A	3200	1.30
PVP ₆₂	100	29	3223	6900	1.32

^a Sample names are determined according to the number average degree of polymerisation (DP) determined by SEC; ^b Monomer to RAFT agent molar ratio; ^c Determined by ¹H NMR using mesitylene as an internal standard; ^d Determined by targeted MW multiplied by conversion; ^e Determined by SEC; ^f Conversion could not be determined as the initial timepoint NMR was not sufficiently concentrated to show the vinyl peaks with reliable integration values.

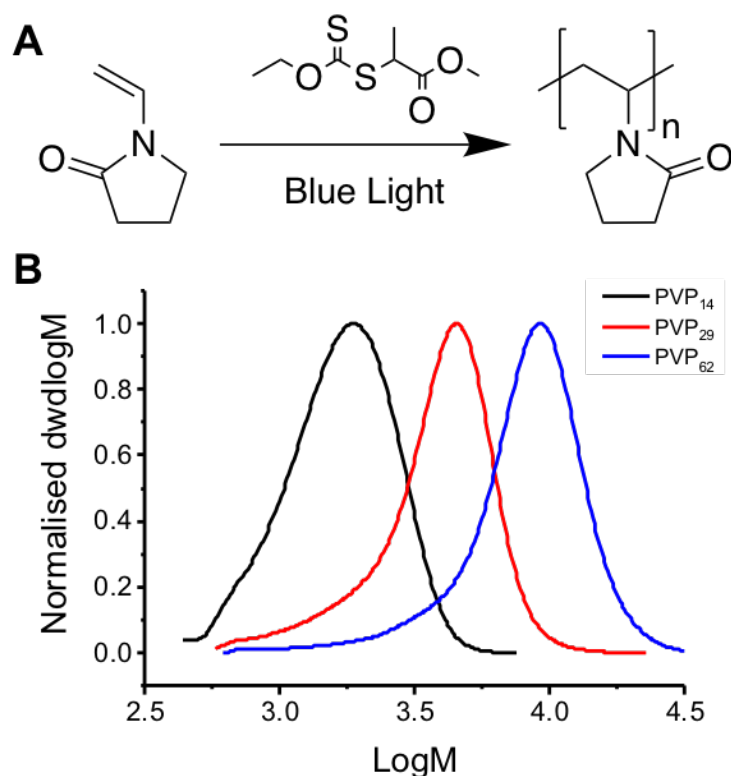


Figure 1. Synthesis and SEC of PVPs. A) Synthetic route used, solvent free in bulk; B) SEC traces of polymers in Table 1.

To evaluate the intrinsic IRI (ice recrystallisation inhibition) activity of PVP the splat assay was used.^{26,35} In short, this involves seeding a polynucleated wafer of small ice crystals (<10 μm) which are then annealed at $-8\text{ }^\circ\text{C}$ for 30 minutes, before their size (growth) is measured relative to a PBS control (Figure 2). A negative control of poly(ethylene glycol) was used to rule out colligative effects, as high concentrations of any polymer will also limit the rate of ice growth (See ESI). At both 10 and 20 $\text{mg}\cdot\text{mL}^{-1}$, none of the polymers demonstrated significant IRI activity, which presented the opportunity to explore if IRI activity can be induced by the increase of hydrophobicity (Figure 3). It is important to highlight very few materials have IRI activity, and several recent reviews summarise these.^{5,18,19}

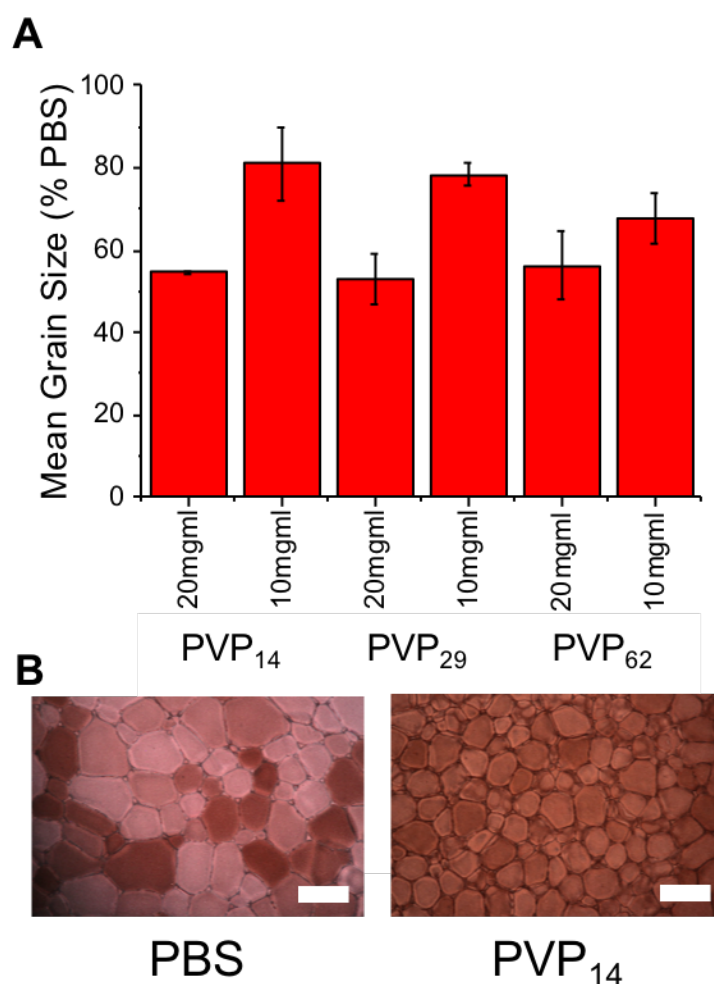


Figure 2. IRI activity of PVP homopolymers. A) IRI activity data of homo PVPs, expressed as MGS (mean grain size) relative to a PBS control. Errors bars are \pm S.D, $n = 3$; B)

Example ice wafers. A PBS control is shown on the left, and a sample containing the PVP₁₄ polymer at 20 mgml⁻¹ on the right, both after 30 minutes of annealing. Scale bars are 100 μm. MGS = mean grain size.

The main aim of this work was to evaluate the impact of hydrophobic comonomers on IRI activity. Therefore, vinyl acetate (VAc) was copolymerised with PVP, targeting an overall DP of 100, with VAc content from 5 to 15 mol %. VAc was chosen as it is also a less activated monomer (LAM), and suitable for xanthate copolymerisation,^{26,42} but is also more hydrophobic than PVP. The VAc units also offer a functional handle for post-polymerization modification (described below). ¹H NMR spectroscopy showed that there was some preference for VP over VAc incorporation so the produced polymers may have a gradient like microstructure, expected due the relative reactivity ratios for these monomers (vinyl pyrrolidone $r = 3.30$, vinyl acetate $r = 0.205$), which should discourage extended blocks of VAc when low monomer ratios are used, Table 2.⁵⁷ These polymers were subsequently evaluated for IRI activity as described above. There was a small (but statistically insignificant) increase in the IRI activity (decrease in mean grain size) as the VAc content was increased, which suggested that either copolymerisation cannot introduce more IRI, or that the VAc itself was insufficiently hydrophobic, Figure 3A. Considering these results, a greater degree of introduced hydrophobicity was required to enable this concept to be further probed, Figure 4.

Table 2. PVP-PVAc Copolymer Synthesis

Sample ^a	[VP]:[CTA] ^b (-)	[VAc]:[CTA] ^c (-)	Conv _{VP} ^d (%)	Conv _{VAc} ^e (%)	Mn _{Theo} ^f (g.mol ⁻¹)	Mn _{SEC} ^g (g.mol ⁻¹)	Đ ^g (-)
---------------------	--------------------------------	---------------------------------	--	---	---	--	-----------------------

PVP ₅₂ VAc ₃	90	10	58	29	7300	7000	1.48
PVP ₅₂ VAc ₆	80	20	65	32	6059	6200	1.43
PVP ₅₇ VAc ₁₀	75	25	76	43	7675	6100	1.47

^a Sample names are determined according to the number average degree of polymerisation of each monomer determined by conversion; ^b Vinyl pyrrolidone to RAFT agent molar ratio; ^c Vinyl acetate to RAFT agent molar ratio; ^d Vinyl pyrrolidone conversion determined by ¹H NMR using mesitylene as an internal standard; ^e Vinyl acetate conversion determined by ¹H NMR using mesitylene as an internal standard; ^f Determined by targeted MW multiplied by conversion; ^g Determined by SEC.

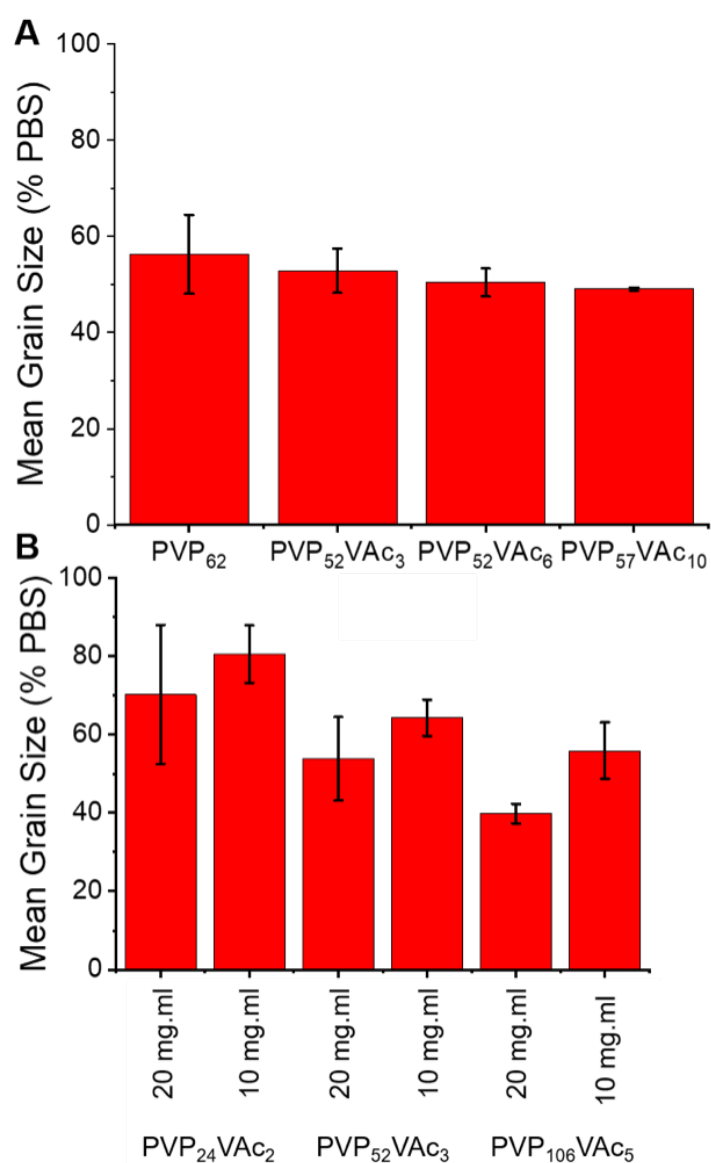


Figure 3. IRI activity of PVP-co-PVAc. A) Impact of VAc content at constant DP, 20 mg.mL⁻¹ ; B) Impact of VAc content on IRI as a function of DP. Error are +/- S.D, n = 3. MGS = mean grain size.

To enable a higher degree of hydrophobicity to be probed, a range of 5 mol% VAc copolymers (with the VAc content limited to ensure the final polymers were water soluble once hydrophobic groups added, to avoid any lower critical solution temperature problems⁵⁴) were synthesised using bulk photopolymerization, as described above, targeting DPs from 50 to 200, shown in Table 3 . The acetate groups were quantitatively removed using hydrazine, as confirmed by ¹H, ¹³C NMR and infrared spectroscopy through the disappearance of the ester carbonyl stretch at ~ 1720 cm⁻¹. The released hydroxyl group was subsequently esterified using a range of acyl chlorides (Figure 4) and functionalisation confirmed by ¹H and ¹³C NMR (Supp Info) generating a library of diversely functionalised PVP copolymers.

Table 3. PVP/PVAc polymer synthesis

Sample ^a	[VP]:[CTA] ^b (-)	[VAc]:[CTA] ^c (-)	Conv _{VVP} ^d (%)	Conv _{VVAc} ^e (%)	Mn _{Theo} ^f (g.mol ⁻¹)	Mn _{SEC} ^g (g.mol ⁻¹)	Đ ^g (-)
PVP ₂₄ VAc ₂	40	10	59%	20%	5700	3600	1.49
PVP ₅₂ VAc ₃	90	10	58%	29%	7300	7000	1.48
PVP ₁₀₆ VAc ₅	190	10	56%	53%	13000	13000	1.65

^a Sample names are determined according to the number average degree of polymerisation of each monomer determined by conversion; ^b Vinyl pyrrolidone to RAFT agent molar ratio; ^c Vinyl acetate to RAFT agent molar ratio; ^d Vinyl pyrrolidone conversion determined by ¹H NMR using mesitylene as an internal standard; ^e Vinyl acetate conversion determined by ¹H NMR using mesitylene as an internal standard; ^f Determined by targeted MW multiplied by conversion; ^g Determined by SEC.

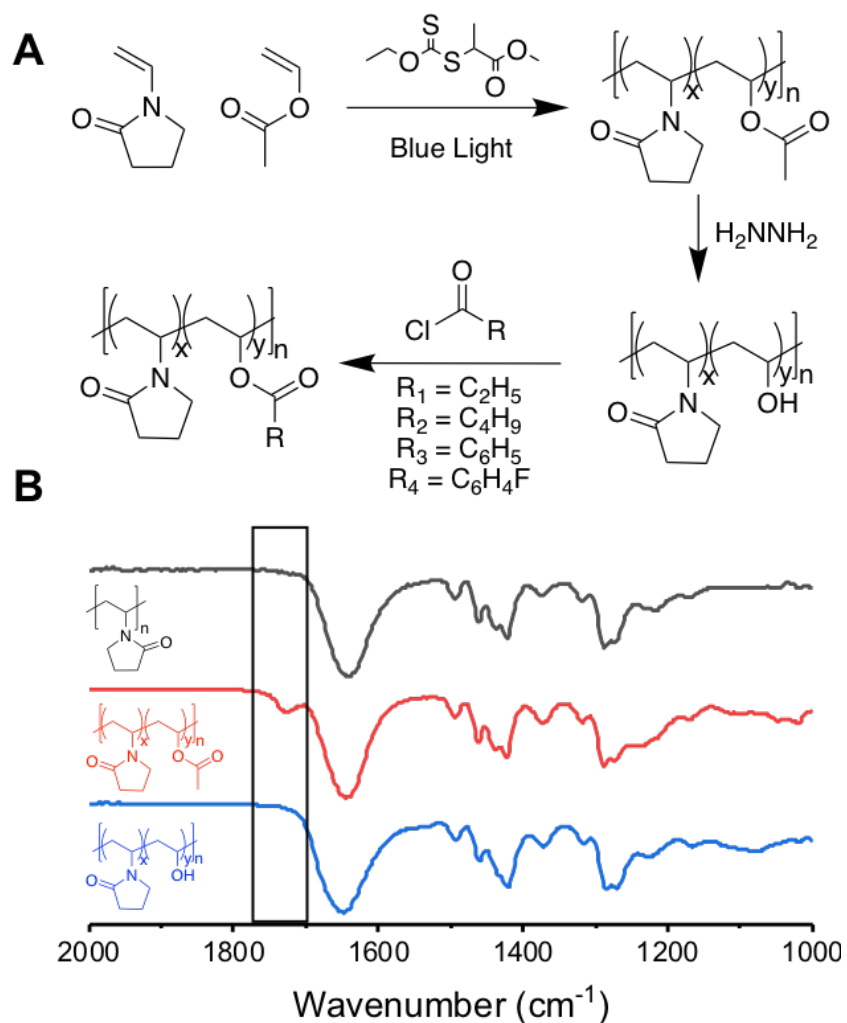


Figure 4. Synthesis of PVP copolymers. A) Synthetic scheme for copolymerisation, followed by deprotection and esterification; B) Infrared spectra showing the introduction of the acetate group, and its subsequent removal after treatment with hydrazine. Vinyl acetate ester unit is highlighted.

The PVP-VAc copolymers described in Table 3 were tested for IRI at both 10 and 20 $mg \cdot mL^{-1}$, and it was observed that the longest polymers (PVP₁₀₆VAc₅) were the most active, leading to 40 % MGS compared to > 60 % for the PVP₆₂ polymers at the higher concentrations. This is consistent with previous observations for polymers and antifreeze glycoproteins, that increasing molecular weight increases activity,^{15,22,26,28} but it should be re-iterated the magnitude of this activity is very low with AFGPs or PVA inhibiting all growth at 1 $mg \cdot mL^{-1}$.

¹. Therefore, only the longest polymers with the hydrophobic modifications were tested, and the results are shown in Figure 5.

Figure 5 A shows the IRI activity of the hydrophobically modified copolymers. In all cases essentially identical IRI activity was observed, independent of the comonomer unit. Plotting the mean grain size at 20 mg.mL⁻¹ against the calculated partition coefficient for the hydrophobic monomer (LogP), showed there was no observable correlation between comonomer hydrophobicity and IRI activity (Figure 5B). These observations are in contrast to what is observed for rigid polymers, such as those derived from ROMP (ring opening metathesis polymerisation) where subtle changes to the hydrophobic unit have a dramatic impact,³² and also in emerging self-assembled systems.^{30,31} This difference has been linked to the need to segregate the hydrophobic units from the hydrophilic to introduce IRI activity. Similar results have been seen in small molecule IRI agents from Ben *et al.*, where in some cases greater hydrophobicity lead to increased IRI,³⁴ but in others it failed to do so. The addition of alkyl chains from one to six carbons did not increase IRI activity, however between seven and sixteen carbon long chains, IRI activity increased and solubility decreased, suggesting a fine balance between hydrophobicity and solubility is required.⁵⁸ When compared to the above results, this suggests that activity cannot be induced in an inactive material simply by the introduction of hydrophobic groups, but that more precise methods are required. Modelling experiments have demonstrated that AGFP binds to ice via its hydrophobic face,²¹ however these results suggest that hydrophobic domains are not enough, and that the 3D presentation and control of these hydrophobic faces is important for the binding of the material to the growing ice face, and therefore the recrystallisation inhibition.

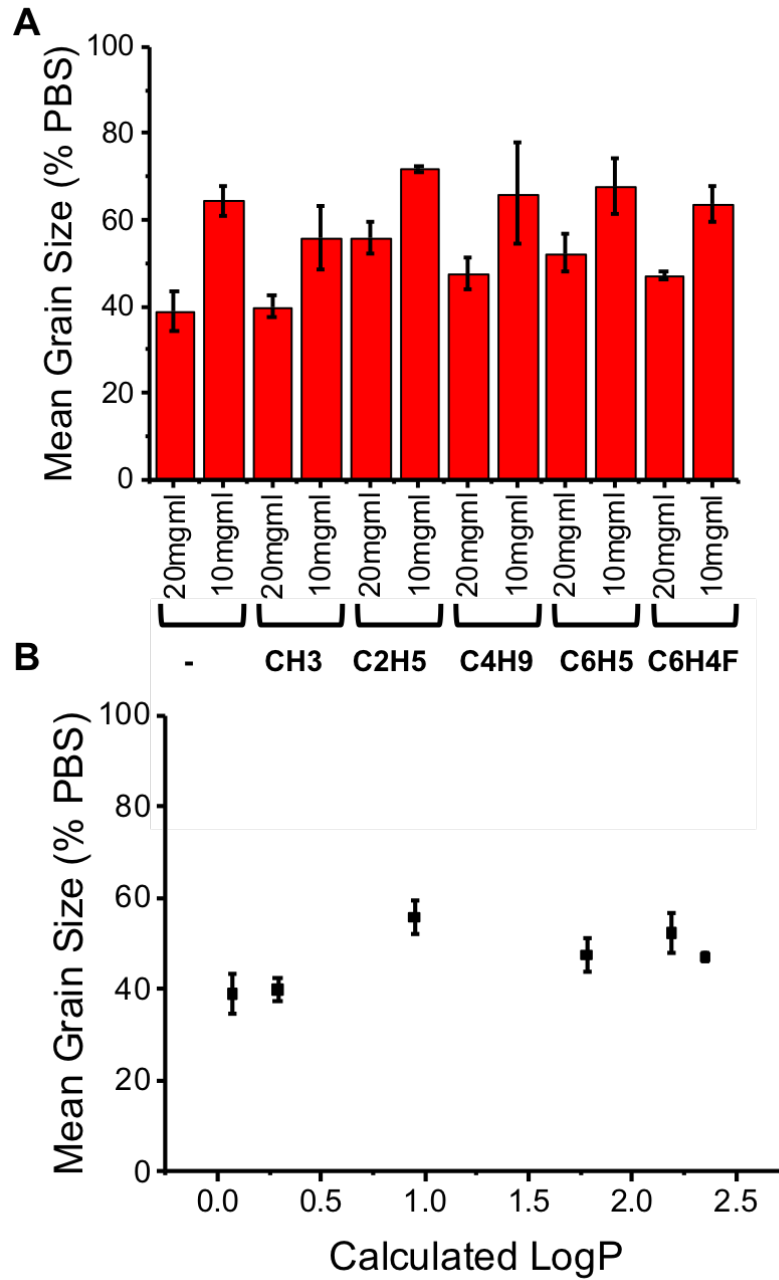


Figure 5. IRI activity of hydrophobically modified PVP copolymers. A) IRI activity of full library; B) Mean grain size verses calculated LogP of the hydrophobic comonomer. MGS = mean grain size.

Conclusions

Herein, the ice growth inhibition potential of poly(vinyl pyrrolidone), as a homopolymer and as a hydrophobically modified copolymer has been sequentially explored. A photopolymerisation method using xanthates as photoinitators/RAFT agents was used, enabling intrinsic blue-light initiated polymerisation in bulk, reaching higher degrees of conversion and lower dispersities than is typically obtained using thermal methods. Copolymers of vinyl acetate (another lesser activated monomer) were also synthesised, which after deprotection enabled sequential side-chain modification of the polymer using a range of acyl chlorides. Ice recrystallisation inhibition assays showed that homo PVP demonstrated no IRI activity compared with negative controls and was therefore a good substrate for further modification. The incorporation of hydrophobic groups failed to lead to any significant increases in activity. This is in contrast to previous reports on rigid-rod polymers and small molecular IRI agents, where introducing hydrophobicity increases activity. These observations support a hypothesis that hydrophobicity alone is not enough to induce ice growth inhibition, and the placement and distribution of the units is crucial. The approach used here did not segregate hydrophobic units, and hence adds support to emerging concepts that the special segregation of the hydrophilic and hydrophobic components is a key feature of all macromolecular IRI agents. These results will help guide the development on next generation of IRI agents, especially focussing efforts towards the development of defined and inflexible copolymers.

Experimental Section

Materials

Phosphate-buffered saline (PBS) solutions were prepared using pre-formulated tablets (Sigma-Aldrich) in 200 mL of Milli-Q water ($>18.2 \Omega$ mean resistivity) to give $[\text{NaCl}] = 0.138 \text{ M}$, $[\text{KCl}] = 0.0027 \text{ M}$, and pH 7.4. Vinyl acetate ($> 99\%$), 2-vinyl pyrrolidone, methyl bromoacetate, fluorobenzoyl chloride, benzoyl chloride, valeroyl chloride, propionyl chloride, polyethylene glycol, mesitylene and hydrazine hydrate solution (78-82 % in water) were purchased from Sigma-Aldrich. Vinyl acetate was filtered through a plug of basic alumina to remove inhibitors prior to use. Potassium ethyl xanthate (98%) was purchased from Alfa Aesar. All solvents were purchased from VWR or Sigma Aldrich and reagents were used without further purification unless indicated.

Physical and Analytical Methods

^1H and ^{13}C NMR spectra were recorded on Bruker Avance III HD 300 MHz, HD 400 MHz or HD 500 MHz spectrometers using deuterated solvents obtained from Sigma-Aldrich. Chemical shifts are reported relative to residual non-deuterated solvent. All size exclusion chromatography (SEC) data were recorded in THF on an Agilent 390-LC MDS instruments equipped with differential refractive index (DRI) detectors. Systems were equipped with 2 x PLgel Mixed C columns (300 x 7.5 mm) and a PLgel 5 μm guard column. The eluents are THF with 2 % TEA (triethylamine) and 0.01 % BHT (butylated hydroxytoluene). All samples were run at $1 \text{ mL}\cdot\text{min}^{-1}$ at 30°C . Poly(methyl methacrylate) standards (Agilent EasyVials) were used for calibration. Analyte samples were filtered through a nylon membrane with $0.22 \mu\text{m}$ pore size before injection. Respectively, experimental molar mass ($M_{n,\text{SEC}}$) and dispersity (D) values of synthesized polymers were determined by conventional calibration using Agilent GPC/SEC software.

Ice wafers were annealed on a Linkam Biological Cryostage BCS196 with T95-Linkpad system controller equipped with a LNP95-Liquid nitrogen cooling pump, using liquid nitrogen as the coolant (Linkam Scientific Instruments UK, Surrey, UK). An Olympus CX41 microscope equipped with a UIS-2 20x/0.45/ ∞ /0-2/FN22 lens (Olympus Ltd, Southend on sea, UK) and a Canon EOS 500D SLR digital camera was used to obtain all images. Image processing was conducted using Image J, which is freely available from <http://imagej.nih.gov/ij/>. LogP was calculated from the hydrophobicity of the pendant group using ChemDraw Professional 16.0.

Ice Recrystallization Inhibition Assay. A 10 μ L droplet of polymer in PBS solution is dropped from 1.4 m onto a glass microscope coverslip, which is on top of an aluminium plate cooled to -78 °C using dry ice. The droplet freezes instantly upon impact with the plate, spreading out and forming a thin wafer of ice. This wafer is then placed on a liquid nitrogen cooled cryostage held at -8 °C. The wafer is then left to anneal for 30 minutes at -8 °C. The number of crystals in the image is counted, again using ImageJ, and the area of the field of view divided by this number of crystals to give the average crystal size per wafer, and reported as a % of area compared to PBS control.

Synthesis of PVP homopolymers

As a representative example, 2-vinyl pyrrolidone (1 g, 9 mmol, 100 eq), CTA 1 (0.018 g, 0.09 mmol, 1 eq) and Mesitylene (20 μ L) were added to a 20ml vial and sealed with a subaseal. The solution was degassed and a sample taken for ^1H NMR. The vial was wrapped with blue LEDs and left to react for 24 hours. After which, another sample was taken for NMR, and conversion determined by analysing the mesitylene standard. The resulting

polymer was precipitated three times into hexane, dried and dissolved in water, followed by lyophilisation to evolve a fine white powder.

^1H NMR (400 MHz, CDCl_3): δ = 1.39-1.83 ($\text{CH}_2\text{CH}(\text{C}_4\text{H}_6\text{NO})$, br, 2H), 1.84-2.07 ($\text{NCH}_2\text{CH}_2\text{CH}_2\text{CO}$, br, 2H), 2.08-2.50 ($\text{NCH}_2\text{CH}_2\text{CH}_2\text{CO}$, br, 2H), 2.93-3.38 ($\text{NCH}_2\text{CH}_2\text{CH}_2\text{CO}$, br, 2H), 3.41-3.86 ($\text{CH}_2\text{CH}(\text{C}_4\text{H}_6\text{NO})$, br 1H). ^{13}C NMR (400 MHz, CDCl_3): δ = 17 ($\text{NCH}_2\text{CH}_2\text{CH}_2\text{CO}$), 31 ($\text{NCH}_2\text{CH}_2\text{CH}_2\text{CO}$), 35 ($\text{CH}_2\text{CH}(\text{C}_4\text{H}_6\text{NO})$), 44 ($\text{NCH}_2\text{CH}_2\text{CH}_2\text{CO}$), 52 ($\text{CH}_2\text{CH}(\text{C}_4\text{H}_6\text{NO})$), 177 ($\text{NCH}_2\text{CH}_2\text{CH}_2\text{CO}$). IR Lactam C=O 1642 cm^{-1} . $M_n^{\text{SEC}}(\text{DMF}) = 6,900$ Da, $M_w/M_n = 1.32$.

Synthesis of PVP-PVAc copolymers

As a representative example, 2-vinyl pyrrolidone (1 g, 9 mmol, 90 eq), vinyl acetate (0.086 g, 1 mmol, 10 eq), CTA 1 (0.02 g, 0.1 mmol) and Mesitylene (20 μL) were added to a 20ml vial and sealed with a subaseal. The solution was degassed and a sample taken for ^1H NMR. The vial was wrapped with blue LEDs and left to react for 24 hours. At the end of the reaction, another sample was taken for NMR, and conversion determined by analysing the mesitylene standard. The resulting polymer was precipitated three times into hexane, dried and dissolved in water, followed by lyophilisation to evolve a fine white powder.

^1H NMR (400 MHz, CDCl_3): δ = 1.39-1.84 ($\text{CH}_2\text{CH}(\text{C}_4\text{H}_6\text{NO})$, $\text{CH}_2\text{CH}(\text{O})\text{CH}_2$, br), 1.86-2.09 ($\text{NCH}_2\text{CH}_2\text{CH}_2\text{CO}$, CH_3COOCH , br), 2.10-2.53 ($\text{NCH}_2\text{CH}_2\text{CH}_2\text{CO}$, br), 2.93-3.39 ($\text{NCH}_2\text{CH}_2\text{CH}_2\text{CO}$, br), 3.40-3.93 ($\text{CH}_2\text{CH}(\text{C}_4\text{H}_6\text{NO})$, br), 4.51-4.63 ($\text{CH}_3\text{CH}(\text{O})\text{CH}_2$, br). ^{13}C NMR (400 MHz, CDCl_3): δ = 16 ($\text{CH}_2\text{CHOCOCH}_3$), 17($\text{NCH}_2\text{CH}_2\text{CH}_2\text{CO}$), 31 ($\text{NCH}_2\text{CH}_2\text{CH}_2\text{CO}$), 35 ($\text{CH}_2\text{CH}(\text{C}_4\text{H}_6\text{NO})$), 42 ($\text{NCH}_2\text{CH}_2\text{CH}_2\text{CO}$), 44 ($\text{CH}_2\text{CHOCOCH}_3$), 45 ($\text{CH}_2\text{CH}(\text{C}_4\text{H}_6\text{NO})$), 97 ($\text{CH}_2\text{CHOCOCH}_3$), 177 ($\text{NCH}_2\text{CH}_2\text{CH}_2\text{CO}$), 178 (CH_3COO). IR Lactam C=O 1646 cm^{-1} , Acetate C=O 1729 cm^{-1} . $M_n^{\text{SEC}}(\text{DMF}) = 7,000$ Da, $M_w/M_n = 1.48$.

Deprotection of PVP-PVAc Copolymers

Poly(2-vinyl pyrrolidone-*co*-vinyl acetate) (0.5 g) was added to a round bottom flask and dissolved in methanol (10 mL) with stirring. The flask was heated to 50 °C and hydrazine (10 mL) added. The reaction was left for 24 hours, after which the solvent was concentrated *in vacuo* and the polymer/methanol solution precipitated into diethyl ether. Solvent was removed and the sample dissolved in water followed by lyophilisation to produce a fine white powder.

¹H NMR (400 MHz, CDCl₃): δ = 1.27-1.80 (CH₂CH(C₄H₆NO), CH₂CHOH, br), 1.80-2.07 (NCH₂CH₂CH₂CO, br), 2.09-2.58 (NCH₂CH₂CH₂CO, br), 2.83-3.39 (NCH₂CH₂CH₂CO, br), 3.40-3.93 (CH₂CH(C₄H₆NO), CH₂CHOH, br). ¹³C NMR (400 MHz, CDCl₃): δ = 18 (NCH₂CH₂CH₂CO), 31 (NCH₂CH₂CH₂CO), 34 (CH₂CH(C₄H₆NO), 42 (NCH₂CH₂CH₂CO), 44 (CH₂CH(C₄H₆NO), 46 (CH₂CHOH), 119 (CH₂CHOH), 177 (NCH₂CH₂CH₂CO). IR Lactam C=O 1648 cm⁻¹. M_n^{SEC}(DMF) = 4,100 Da, M_w/M_n = 3.33.

Functionalisation of PVP-PVA Copolymers

Benzoyl Chloride - Poly(vinyl pyrrolidone-*co*-vinyl alcohol) (150 mg) was dissolved in dimethylformamide (10 mL) with stirring and left to dissolve. After 30 minutes, triethylamine (20 mg) and benzoyl chloride (45 mg) was added and left to react for 3 hours. After which the polymer was concentrated *in vacuo* and precipitated into diethyl ether (x3) and dried under vacuum. The polymer was then dissolved in water and purified using centrifugal dialysis (3k MWCO, Millipore) followed by lyophilisation.

¹H NMR (400 MHz, D₂O): δ = 1.29-1.84 (CH₂CH(C₄H₆NO), CH₂CHOCO, br), 1.85-2.09 (NCH₂CH₂CH₂CO, br), 2.10-2.53 (NCH₂CH₂CH₂CO, br), 2.91-3.41 (NCH₂CH₂CH₂CO, br), 3.42-4.18 (CH₂CH(C₄H₆NO), CH₂CHOCO, br), 7.44-7.55 (meta-CH, br), 7.57-7.65 (para-CH, br), 7.72-7.83 (ortho-CH, br).

4-Fluorobenzoyl Chloride - Poly(vinyl pyrrolidone-*co*-vinyl alcohol) (150 mg) was dissolved in dimethylformamide (10 mL) with stirring and left to dissolve. After 30 minutes, triethylamine (20 mg) and 4-fluorobenzoyl chloride (55 mg) was added and left to react for 3 hours. After which the polymer was concentrated *in vacuo* and precipitated into diethyl ether (x3) and dried under vacuum. The polymer was then dissolved in water and purified using centrifugal dialysis (3k MWCO, Millipore) followed by lyophilisation.

¹H NMR (400 MHz, D₂O): δ = 1.30-1.84 (*CH*₂*CH*(C₄H₆NO), *CH*₂*CHOCO*, br), 1.85-2.08 (N*CH*₂*CH*₂*CH*₂*CO*, br), 2.09-2.60 (N*CH*₂*CH*₂*CH*₂*CO*, br), 2.96-3.39 (N*CH*₂*CH*₂*CH*₂*CO*, *CH*₂*CHO* br), 3.40-4.09 (*CH*₂*CH*(C₄H₆NO), *CH*₂*CHOCO*, br), 7.10-7.30 (meta-*CH*, br), 7.75-7.90 (ortho-*CH*, br). ¹⁹F NMR decoupled (400 MHz, D₂O): δ = -106 (para-CF, s, 1F)

Propionyl Chloride - Poly(vinyl pyrrolidone-*co*-vinyl alcohol) (150 mg) was dissolved in dimethylformamide (10 mL) with stirring and left to dissolve. After 30 minutes, triethylamine (20 mg) and propionyl chloride (30 mg) was added and left to react for 3 hours. After which the polymer was concentrated *in vacuo* and precipitated into diethyl ether (x3) and dried under vacuum. The polymer was then dissolved in water and purified using centrifugal dialysis (3k MWCO, Millipore) followed by lyophilisation.

¹H NMR (400 MHz, D₂O): δ = 1.34-1.85 (*CH*₂*CH*(C₄H₆NO), *CH*₂*CHOCO*, br), 1.86-2.07 (N*CH*₂*CH*₂*CH*₂*CO*, br), 2.09-2.59 (N*CH*₂*CH*₂*CH*₂*CO*, *CH*₃*CH*₂*COO* br), 2.90-3.38 (N*CH*₂*CH*₂*CH*₂*CO*, *CH*₂*CHO* br), 3.40-4.10 (*CH*₂*CH*(C₄H₆NO), *CH*₂*CHOCO*, *CH*₃*CH*₂*COO*, br). ¹³C NMR (400 MHz, D₂O): δ = 18 (N*CH*₂*CH*₂*CH*₂*CO*, *CH*₃*CH*₂*COO*), 32 (N*CH*₂*CH*₂*CH*₂*CO*), 34 (*CH*₂*CHOCO*, *CH*₂*CH*(C₄H₆NO)), 42 (N*CH*₂*CH*₂*CH*₂*CO*), 44 (*CH*₂*CH*(C₄H₆NO), 46 (*CH*₂*CHOCO*), 62 (*CH*₃*CH*₂*COO*), 177 (*CH*₃*CH*₂*COO*, N*CH*₂*CH*₂*CH*₂*CO*).

Valeroyl Chloride - Poly(vinyl pyrrolidone-*co*-vinyl alcohol) (150 mg) was dissolved in dimethylformamide (10 mL) with stirring and left to dissolve. After 30 minutes, triethylamine (20 mg) and propionyl chloride (35 mg) was added and left to react for 3 hours. After which the polymer was concentrated *in vacuo* and precipitated into diethyl ether (x3) and dried under vacuum. The polymer was then dissolved in water and purified using centrifugal dialysis (3k MWCO, Millipore) followed by lyophilisation.

^1H NMR (400 MHz, D_2O): δ = 1.35-1.84 ($\text{CH}_2\text{CH}(\text{C}_4\text{H}_6\text{NO})$, CH_2CHOCO , br), 1.83-2.08 ($\text{NCH}_2\text{CH}_2\text{CH}_2\text{CO}$, $\text{CH}_3\text{CH}_2\text{CH}_2\text{COO}$, $\text{CH}_3\text{CH}_2\text{CH}_2\text{COO}$, br), 2.09-2.67 ($\text{NCH}_2\text{CH}_2\text{CH}_2\text{CO}$, $\text{CH}_3\text{CH}_2\text{COO}$ br), 2.90-3.37 ($\text{NCH}_2\text{CH}_2\text{CH}_2\text{CO}$, CH_2CHO br), 3.39-4.10 ($\text{CH}_2\text{CH}(\text{C}_4\text{H}_6\text{NO})$, CH_2CHOCO , $\text{CH}_3\text{CH}_2\text{CH}_2\text{COO}$, br). ^{13}C NMR (400 MHz, D_2O): δ = 17 ($\text{CH}_3\text{CH}_2\text{CH}_2\text{COO}$, $\text{CH}_3\text{CH}_2\text{CH}_2\text{COO}$, $\text{NCH}_2\text{CH}_2\text{CH}_2\text{CO}$), 32 ($\text{NCH}_2\text{CH}_2\text{CH}_2\text{CO}$), 34 (CH_2CHOCO , $\text{CH}_2\text{CH}(\text{C}_4\text{H}_6\text{NO})$), 42 ($\text{NCH}_2\text{CH}_2\text{CH}_2\text{CO}$), 44 ($\text{CH}_2\text{CH}(\text{C}_4\text{H}_6\text{NO})$), 46 (CH_2CHOCO), 63 ($\text{CH}_3\text{CH}_2\text{COO}$), 177 ($\text{CH}_3\text{CH}_2\text{CH}_2\text{COO}$, $\text{NCH}_2\text{CH}_2\text{CH}_2\text{CO}$).

Acknowledgements

M.I.G. holds an ERC starting grant (CRYOMAT 638661). The Royal Society are also thanked for funding the cryo-microscopes used in this study. We are grateful for the polymer characterization RTP for size- exclusion chromatography support.

Data Availability Statement

The processed data required to reproduce these findings are available to download from the Warwick Research Repository <http://wrap.warwick.ac.uk/>

References

- 1 O. Parent and A. Ilinca, *Cold Reg. Sci. Technol.*, 2011, **65**, 88–96.
- 2 W. O. Valarezo, F. T. Lynch and R. J. McGhee, *J. Aircr.*, 1993, **30**, 807–812.
- 3 G. John Morris and E. Acton, *Cryobiology*, 2013, **66**, 85–92.
- 4 A. Fowler and M. Toner, *Ann. N. Y. Acad. Sci.*, 2005, **1066**, 119–135.
- 5 Z. He, K. Liu and J. Wang, *Acc. Chem. Res.*, 2018, **51**, 1082–1091.
- 6 L. R. Maki, E. L. Galyan, M. M. Chang-Chien and D. R. Caldwell, *Appl. Microbiol.*, 1974, **28**, 456–459.
- 7 K. Dreischmeier, C. Budke, L. Wiehemeier, T. Kottke and T. Koop, *Sci. Rep.*, 2017, **7**, 41890.
- 8 R. N. Ben, *ChemBioChem*, 2001, **2**, 161–166.
- 9 A. K. Balcerzak, C. J. Capicciotti, J. G. Briard and R. N. Ben, *RSC Adv.*, 2014, **4**, 42682–42696.
- 10 P. Mazur, *Science (80-.)*, 1970, **168**, 939–949.
- 11 C. Koshimoto and P. Mazur, *Cryobiology*, 2002, **45**, 49–59.
- 12 E. Bender, *Nature*, 2016, **540**, S106–S108.
- 13 J. G. Baust, D. Gao and J. M. Baust, *Organogenesis*, 2009, **5**, 90–96.
- 14 J. G. Baust, D. Gao and J. M. Baust, *Organogenesis*, 2009, **5**, 90–96.
- 15 B. Graham, T. L. Bailey, J. R. J. Healey, M. Marcellini, S. Deville and M. I. Gibson, *Angew. Chem. Int. Ed.*, 2017, **56**, 15941–15944.
- 16 J. Lee, E.-W. Lin, U. Y. Lau, J. L. Hedrick, E. Bat and H. D. Maynard, *Biomacromolecules*, 2013, **14**, 2561–9.
- 17 M. Hasan, A. E. R. Fayter and M. I. Gibson, *Biomacromolecules*, 2018, **19**, 3371–3376.
- 18 C. I. Biggs, T. L. Bailey, Ben Graham, C. Stubbs, A. Fayter and M. I. Gibson, *Nat.*

- Commun.*, 2017, **8**, 1546.
- 19 I. K. Voets, *Soft Matter*, 2017, **13**, 4808–4823.
 - 20 M. I. Gibson, *Polym. Chem.*, 2010, **1**, 1141–1152.
 - 21 K. Mochizuki and V. Molinero, *J. Am. Chem. Soc.*, 2018, **140**, 4803–4811.
 - 22 C. Budke, A. Dreyer, J. Jaeger, K. Gimpel, T. Berkemeier, A. S. Bonin, L. Nagel, C. Plattner, A. L. Devries, N. Sewald and T. Koop, *Cryst. Growth Des.*, 2014, **14**, 4285–4294.
 - 23 C. P. Garnham, R. L. Campbell and P. L. Davies, *Proc. Natl. Acad. Sci.*, 2011, **108**, 7363–7367.
 - 24 A. Wierzbicki, P. Dalal, T. E. Cheatham, J. E. Knickelbein, A. D. J. Haymet and J. D. Madura, *Biophys. J.*, 2007, **93**, 1442–51.
 - 25 E. I. Howard, M. P. Blakeley, M. Haertlein, I. P. Haertlein, A. Mitschler, S. J. Fisher, A. C. Siah, A. G. Salvay, A. Popov, C. M. Dieckmann, T. Petrova and A. Podjarny, *J. Mol. Recognit.*, 2011, **24**, 724–732.
 - 26 T. Congdon, R. Notman and M. I. Gibson, *Biomacromolecules*, 2013, **14**, 1578–1586.
 - 27 T. Inada and S. S. Lu, *Cryst. Growth Des.*, 2003, **3**, 747–752.
 - 28 C. Budke and T. Koop, *ChemPhysChem*, 2006, **7**, 2601–2606.
 - 29 P. M. Naullage, L. Lupi and V. Molinero, *J. Phys. Chem. C*, 2017, **121**, 26949–26957.
 - 30 R. Drori, C. Li, C. Hu, P. Raiteri, A. Rohl, M. D. Ward and B. Kahr, *J. Am. Chem. Soc.*, 2016, **138**, 13396–13401.
 - 31 D. E. Mitchell, G. Clarkson, D. J. Fox, R. A. Vipond, P. Scott and M. I. Gibson, *J. Am. Chem. Soc.*, 2017, **139**, 9835–9838.
 - 32 B. Graham, A. E. R. Fayter, J. E. Houston, R. C. Evans and M. I. Gibson, *J. Am. Chem. Soc.*, 2018, **140**, 5682–5685.
 - 33 M. I. Gibson, C. A. Barker, S. G. Spain, L. Albertin and N. R. Cameron, *Biomacromolecules*, 2009, **10**, 328–333.

- 34 C. J. Capicciotti, M. Leclere, F. A. Perras, D. L. Bryce, H. Paulin, J. Harden, Y. Liu and R. N. Ben, *Chem. Sci.*, 2012, **3**, 1408–1416.
- 35 A. K. Balcerzak, M. Febbraro and R. N. Ben, *RSC Adv.*, 2013, **3**, 3232–3236.
- 36 P. Czechura, R. Y. Tam, E. Dimitrijevic, A. V. Murphy and R. N. Ben, *J. Am. Chem. Soc.*, 2008, **130**, 2928–2929.
- 37 A. Kiselev, F. Bachmann, P. Pedevilla, S. J. Cox, A. Michaelides, D. Gerthsen and T. Leisner, *Science (80-.)*, 2016, 355, 1–10.
- 38 Q. Zhang and M. A. Kelland, *Energy & Fuels*, 2018, **32**, acs.energyfuels.8b01985.
- 39 M. A. Kelland, *Energy and Fuels*, 2006, 20, 825–847.
- 40 S. Harrisson, X. Liu, J.-N. Ollagnier, O. Coutelier, J.-D. Marty and M. Destarac, *Polymers (Basel)*, 2014, **6**, 1437–1488.
- 41 Q. Liu, H. Wu, L. Zhang, Y. Zhou, W. Zhang, X. Pan, Z. Zhang and X. Zhu, *Polym. Chem.*, 2016, **7**, 2015–2021.
- 42 M. H. Stenzel, L. Cummins, G. E. Roberts, T. P. Davis, P. Vana and C. Barner-Kowollik, *Macromol. Chem. Phys.*, 2003, **204**, 1160–1168.
- 43 S. Perrier, *Macromolecules*, 2017, **50**, 7433–7447.
- 44 N. Corrigan, J. Yeow, P. Judzewitsch, J. Xu and C. A. J. M. Boyer, *Angew. Chem. Int. Ed.*, 2018.
- 45 M. Y. Khan, M.-S. Cho and Y.-J. Kwark, *Macromolecules*, 2014, **47**, 1929–1934.
- 46 J. Xu, K. Jung, A. Atme, S. Shanmugam and C. Boyer, *J. Am. Chem. Soc.*, 2014, **136**, 5508–5519.
- 47 S.-J. Richards, A. Jones, R. M. Thomás and M. I. Gibson, *Chem. - A Eur. J.*, 2018, **doi: 10.10**.
- 48 R. Chapman, A. J. Gormley, M. H. Stenzel and M. M. Stevens, *Angew. Chem. Int. Ed. Engl.*, 2016, **55**, 4500–3.
- 49 J. Yeow, R. Chapman, J. Xu and C. Boyer, *Polym. Chem.*, 2017, **8**, 5012–5022.

- 50 D. Britton, F. Heatley and P. A. Lovell, *Macromolecules*, 1998, **31**, 2828–2837.
- 51 Q. Fu, K. Xie, T. G. McKenzie and G. G. Qiao, *Polym. Chem.*, 2017, **8**, 1519–1526.
- 52 C. A. Figg, J. D. Hickman, G. M. Scheutz, S. Shanmugam, R. N. Carmean, B. S. Tucker, C. Boyer and B. S. Sumerlin, *Macromolecules*, 2018, **51**, 1370–1376.
- 53 C. Ding, C. Fan, G. Jiang, X. Pan, Z. Zhang, J. Zhu and X. Zhu, *Macromol. Rapid Commun.*, 2015, **36**, 2181–2185.
- 54 N. S. Jeong, M. Redhead, C. Bosquillon, C. Alexander, M. Kelland and R. K. O'Reilly, *Macromolecules*, 2011, **44**, 886–893.
- 55 N. S. Jeong, K. Brebis, L. E. Daniel, R. K. O'Reilly and M. I. Gibson, *Chem. Commun.*, 2011, **47**, 11627–11629.
- 56 N. S. Jeong, M. Hasan, D. J. Phillips, Y. Saaka, R. K. O'Reilly and M. I. Gibson, *Polym. Chem.*, 2012, **3**, 794–799.
- 57 J. F. Bork and L. E. Coleman, *J. Polym. Sci.*, 2003, **43**, 413–421.
- 58 A. K. Balcerzak, C. J. Capicciotti, J. G. Briard and R. N. Ben, *RSC Adv.*, 2014, **4**, 42682–42696.